Neuroepithelial body microenvironment is a niche for a distinct subset of Clara-like precursors in the developing airways

Arjun Guha[a,1,2], Michelle Vasconcelos[a,1], Yan Cai[b], Mitsuhiro Yoneda[b], Anne Hinds[a], Jun Qian[a], Guihua Li[a], Lauren Dickel[c], Jane E. Johnson[c], Shioko Kimura[b], Jinjin Guo[d], Jill McMahon[d], Andrew P. McMahon[d], and Wellington V. Cardoso[a,2]

[a]Pulmonary Center, Department of Medicine, Boston University School of Medicine, Boston, MA 02118; [b]Laboratory of Metabolism, National Cancer Institute, Bethesda, MD 20892; [c]Department of Neuroscience, University of Texas Southwestern Medical Center, Dallas, TX 75390; and [d]Department of Molecular and Cell Biology, Harvard University, Cambridge, MA 01238

Edited* by Brigid L. M. Hogan, Duke University Medical Center, Durham, NC, and approved May 21, 2012 (received for review March 26, 2012)

Clara cells of mammalian airways have multiple functions and are morphologically heterogeneous. Although Notch signaling is essential for the development of these cells, it is unclear how Notch influences Clara cell specification and if diversity is established among Clara cell precursors. Here we identify expression of the secretoglobin *Scgb3a2* and Notch activation as early events in a program of secretory cell fate determination in developing murine airways. We show that *Scgb3a2* expression in vivo is Notch-dependent at early stages and ectopically induced by constitutive Notch1 activation, and also that in vitro Notch signaling together with the pan-airway transcription factor Ttf1 (Nkx2.1) synergistically regulate secretoglobin gene transcription. Furthermore, we identified a subpopulation of secretory precursors juxtaposed to presumptive neuroepithelial bodies (NEBs), distinguished by their strong *Scgb3a2* and *uroplakin 3a* (*Upk3a*) signals and reduced Ccsp (Scgb1a1) expression. Genetic ablation of *Ascl1* prevented NEB formation and selectively interfered with the formation of this subpopulation of cells. Lineage labeling of *Upk3a*-expressing cells during development showed that these cells remain largely uncommitted during embryonic development and contribute to Clara and ciliated cells in the adult lung. Together, our findings suggest a role for Notch in the induction of a Clara cell-specific program of gene expression, and reveals that the NEB microenvironment in the developing airways is a niche for a distinct subset of Clara-like precursors.

The airways of the mammalian lung are populated by distinct epithelial cell types distinguished by their morphology and expression of molecular markers. Clara and ciliated cells are the most abundant, whereas basal and neuroendocrine (NE) cells are restricted in number and distribution (1). Clara cells synthesize components of the airway lining fluid, mediate mucociliary clearance in concert with ciliated cells, metabolize environmental toxins, and act as facultative progenitor cells during lung injury repair (1–3).

Clara cells in the mouse lung have been distinguished in molecular terms by the expression of the secretoglobin Scgb1a1/Clara cell secretory protein (Ccsp or CC10). Subpopulations of Clara cells with distinctive morphology and susceptibility to environmental exposures have been reported in the mouse lung and in other species (4). For example, ultrastructural analysis of conducting airways shows that Clara cells surrounding clusters of neuroepithelial cells [neuroepithelial bodies (NEBs)] have a distinct flattened morphology (5). These cells are also functionally distinct from other Clara cells because they are deficient in the cytochrome P450 enzyme Cyp2f2 (6). It is thought that the absence of Cyp2f2 renders resistance to naphthalene injury (6).

Genetic studies in mice demonstrate an essential role for the Notch signaling in the specification of Clara cells during lung development (7, 8). The Notch pathway is a juxtacrine signaling system that regulates cell fate choices in multiple organisms (9–11). The pathway is activated by the binding of transmembrane Notch receptors (Notch1–4) and transmembrane ligands Delta-like (Dll1, Dll3, Dll4) or Jagged (Jag1, Jag2). Ligand–receptor interaction results in γ-secretase–dependent cleavage of the cytoplasmic domain of the Notch receptor. Nuclear translocation and interaction of this cleaved intracellular domain (NICD) with the Rbpjk transcriptional complex then leads to activation of a canonical pathway and the expression of target genes. Developing airways that are deficient in Rbpjk or protein *O*-fucosyltransferase-1 (Pofut1), an enzyme required for the efficient binding of Notch receptor to ligand, lack Clara cells and have supernumerary ciliated cells (7, 8). Conversely, constitutive activation in the embryonic lung epithelium results in mucous metaplasia and in a decrease in number of ciliated cells (12).

Studies of the mechanisms of Clara cell specification and the role of Notch signaling therein have been limited by the paucity of early markers of differentiation. Transcription factors that label ciliated (Foxj1), neuroendocrine (Ascl1), and basal (Trp63) progenitors are known. However, with the exception of NICD, no nuclear factor specific to Clara cell progenitors has been identified. Hes1, a Notch transcriptional target, is expressed broadly in developing airways, but is not required for the specification of Clara cells (13). Secretoglobins are a family of small, secreted, structurally similar disulfide-linked dimers of which three members, Ccsp (Scgb1a1), Scgb3a1, and Scgb3a2, are expressed in Clara cells in the lung (14). At present, the secretoglobin Ccsp is the only definitive marker for Clara cells. Markers, such as Trp63, Ascl1, and Foxj1 have been localized to the developing airways well before the onset of, Ccsp expression at embryonic day 15.5 (E15.5) (14–16).

Here we examined the early events associated with the induction of Clara cell fate and the contribution of developmental programming in establishing differences among Clara cells in the mouse airway epithelium. We identify activated Notch1 and *Scgb3a2* as markers of an early program of Clara cell fate. Moreover, we implicate Notch as a mediator of a Clara cell-specific program of gene expression in airway epithelial precursors. This program is modified in the developing NEB microenvironment to generate a distinct subpopulation of Clara cell precursors.

Author contributions: A.G., Y.C., M.Y., S.K., and W.V.C. designed research; A.G., M.V., Y.C., M.Y., A.H., J.Q., G.L., L.D., and J.M. performed research; A.G., M.V., A.H., J.E.J., J.G., J.M., and A.P.M. contributed new reagents/analytic tools; A.G., J.E.J., S.K., and W.V.C. analyzed data; and A.G. and W.V.C. wrote the paper.

The authors declare no conflict of interest.

*This Direct Submission article had a prearranged editor.

[1]A.G. and M.V. contributed equally to this work.

[2]To whom correspondence may be addressed. E-mail: wcardoso@bu.edu or aguha@bu.edu.

This article contains supporting information online at www.pnas.org/lookup/suppl/doi:10.1073/pnas.1204710109/-/DCSupplemental.

Results

Notch Activation in the Developing Airways Precedes Expression of Known Markers of Airway Differentiation. Lineage analysis of cells that experienced Notch1 activation in the developing airways and loss-of-function genetic studies have shown that Notch signaling correlates with and is essential for Clara cell fate (7, 8). To characterize the spatiotemporal regulation of Notch signaling in the developing airways, we examined the distribution of activated Notch1 by immunohistochemistry (IHC) using an antibody against cleaved Notch1 [referred to hereafter as NICD (7)]. NICD labeling was first detected in the respiratory epithelium at E12.5, at low levels, and restricted to the trachea and main bronchi (Fig. 1 *A* and *B*). At E14.5, NICD-positive cells were more abundant in the proximal airways but absent in the distal airways (Fig. 1 *C–E*). At this stage, strong NICD signals were detected in clusters occupying a relatively apical position within the pseudostratified epithelium in proximal intrapulmonary airways (Fig. 1 *E* and *F*); this contrasted with lower intensity and more homogenous pattern of NICD labeling outside the clusters. The expression in clusters was reminiscent of the distribution of Ascl1 [mouse achaete–scute complex homolog 1 (Mash1)], a bHLH transcription factor essential for NE cell fate and a marker for presumptive neuroepithelial bodies (pNEBs) (15). Double IHC confirmed the presence of the NICD clusters juxtaposed to and distinct from Ascl1-expressing cells (Fig. 1*F*). At this stage most, if not all, clusters of NICD were juxtaposed to pNEBs. By E18.5 NICD was detected throughout the airway epithelium and in clusters associated with pNEBs. (Fig. 1*G*). Previous studies have suggested that Ascl1 (E13.5) is the earliest marker for airway differentiation (15). We conclude that Notch signaling is activated in the developing airway epithelium before any of the known markers of differentiation, and is activated around pNEBs from early stages.

NEB-Associated Cells Show Distinct Phenotypic Features During Development Suggestive of a Subpopulation of Clara Cell Precursors. The early onset of Notch activation in the developing lung suggested that the determination of the Clara cell fate initiates earlier than the expression of Ccsp, and led us to search for early markers. Previous studies report that *Scgb3a2*, another member of the secretoglobin gene family, is also expressed in secretory Clara cells of developing airways (8, 14, 16, 17). We investigated whether *Scgb3a2* correlates with Notch activation at early stages. In situ hybridization (ISH) revealed *Scgb3a2* expression from E12.5 onward; expression was localized to the trachea and extrapulmonary bronchi (Fig. 2*A*). *Scgb3a2* expression became stronger and expanded to lobar bronchi at E13.5–E14.5 and was widespread by E18.5 (Fig. 2 *B–D*). At E14.5, *Scgb3a2* was strongly expressed in clusters of cells in proximal airways (Fig. 2*C*). Double-ISH/IHC and confocal analysis of E14.5 lungs confirmed colocalization of *Scgb3a2* and NICD (Fig. 2*E*). Colocalization was not restricted to these cell clusters but was harder to detect elsewhere in the epithelium due to the weaker NICD signals.

We tested whether clusters of *Scgb3a2*-positive cells were arising at sites of Ascl1-expressing cells, as seen for NICD. Sections from E13.5–E18.5 lungs were labeled with a *Scgb3a2* riboprobe and an anti-Ascl1 antibody. At E14.5, *Scgb3a2* signals were present in the expected uniform and clustered patterns (Fig. 2*F*); 70–80% of the

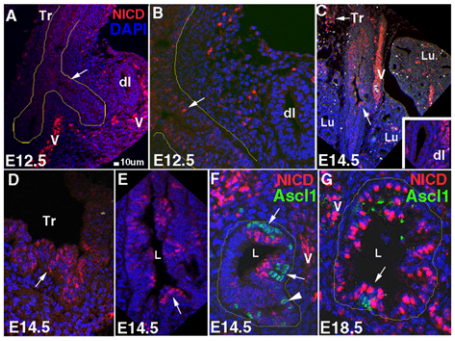

Fig. 1. Spatial pattern of Notch activation in the developing airways. (*A–G*) Labeling for cleaved Notch1 (NICD, red) and Ascl1 (green) indicates that Notch signaling is activated in the airways a few days earlier than Ccsp expression is detected (E15.5, 14), and that it is active in the NEB microenvironment from early stages. (*A* and *B*) Low levels of NICD were detected at E12.5 in trachea (Tr) and main bronchi (arrow), but not in distal (dl) airways (shown at higher resolution in *B*). (*C–F*) At E14.5, NICD labeling was more abundant in both the extrapulmonary airways (Tr in *C*, higher magnification in *D*) and proximal intrapulmonary airways (*C*, higher magnification in *E*), but no labeling was detected in distal airways (*C Inset*). (*F*) Clusters of strong NICD labeling in the proximal airways at E14.5 are associated with clusters of Ascl1-expressing cells (arrows, airway outlined in white). Note the solitary Ascl1-expressing cells (arrowhead) are not associated with strong NICD labeling (*F*). (*G*) At E18.5, widespread labeling of NICD was detected in the intrapulmonary airways, including the NEB microenvironment (arrow). L, lumen; Lu, lung; V, vasculature. (Scale bar: 10 μm.)

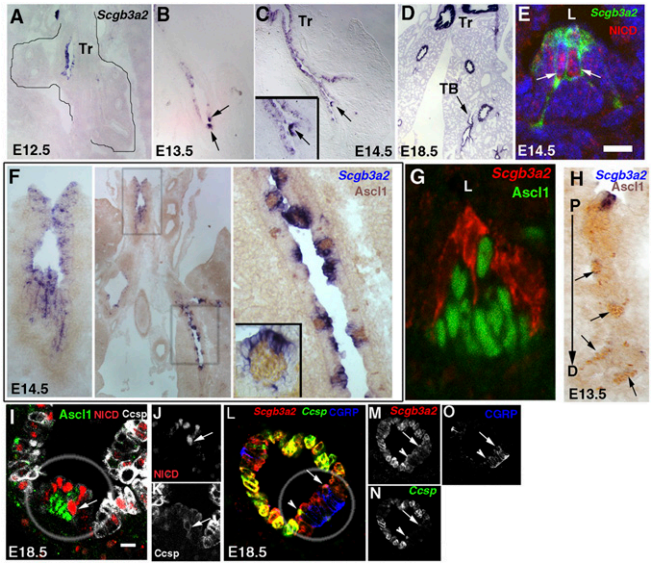

Fig. 2. *Scgb3a2* expression correlates with NICD and identifies a distinct subpopulation of Clara-like progenitors associated with pNEBs. (*A–D*) Time course of *Scgb3a2* expression revealed a pattern similar to that of NICD (Fig. 1). *Scgb3a2* was first detected in the trachea (Tr) at E12.5 (*A*) and in the intrapulmonary airways from E13.5–E14.5 (*B–D*). At E18.5 (*D*), Scgb3a2 expression was widespread and detected in both trachea and terminal bronchiole (TB). Clusters of cells with strong signal could be discerned at E13.5–E14.5 (*B* and *C Inset*, arrows). (*E*) Colocalization of *Scgb3a2* and NICD was readily observed in these cell clusters (arrows; L marks the airway lumen). (*F*) Double-*Scgb3a2* ISH/AscII IHC revealed *Scgb3a2*-labeled clusters (*F Right*) juxtaposed to Ascl1-expressing pNEBs. (*F Right Inset*) *Scgb3a2*-expressing cells (blue) have a clear nucleus not labeled by anti-Ascl1 (brown). No Ascl1-expressing cells were detected in the trachea (*F Left*). (*G*) High-resolution optical section showing that luminal *Scgb3a2*-expressing cells (ISH, red) could be distinguished from basal Ascl1-expressing cells (IHC, green). (*H*) *Scgb3a2* and Ascl1 double-labeling at E13.5 suggests that the formation of Ascl1 clusters (distal, arrows) precedes formation of Scgb3a2-Ascl1 dual clusters. (*I–O*) Analysis of *Ccsp* and *Scgb3a2* expression at E18.5 suggested that the cells associated with pNEBs may be a distinct subpopulation of Clara precursors. (*I–K*) Labeling of NICD (red, shown separately in *J*), Ccsp (white, shown separately in *K*), and Ascl1 (green) showed that the cells in the NEB microenvironment are NICD positive, but express low (arrow)-to-negligible levels of Ccsp at this stage. Cells with both NICD and Ccsp were abundant away from the NEB microenvironment (*I*). (*L–O*) Triple labeling for *Scgb3a2* (ISH, red, shown separately in *M*), Ccsp (ISH, green, shown separately in *N*), and Cgrp (IHC, blue, shown separately in *O*) at E18.5 showed that cells apposed to pNEBs express *Scgb3a2* and low Ccsp (arrowhead), and some have *Scgb3a2* but negligible Ccsp (arrow). Elsewhere, *Scgb3a2* and Ccsp signals are strong and colocalized (*L*).

DEVELOPMENTAL BIOLOGY

Scgb3a2-expressing clusters were associated with the Ascl1-expressing cell clusters. Confocal microscopy confirmed that cells expressing *Scgb3a2* or Ascl1 were distinct and in direct contact (Fig. 2*G*). Interestingly, analysis of E13.5–E14.5 lungs showed a P–D pattern of pNEB formation in intrapulmonary airways, preceding the local appearance of *Scgb3a2* (Fig. 2*H*).

These data showed that the pNEB microenvironment at E14.5 consists of clusters of Ascl1-expressing cells and another cell population expressing high levels of NICD and *Scgb3a2*. No Foxj1 labeling was detected in these cells at any of the stages studied. Therefore, we hypothesized that the NEB microenvironment is a niche for Clara cell precursors and examined the distribution of Ccsp in the NEB microenvironment at E18.5. Simultaneous labeling of NICD/Ccsp/Ascl1 at E18.5 demonstrated that cells clustered around NEBs had high levels of NICD but low-to-negligible levels of Ccsp (Fig. 2 *I–O*). Three-color labeling of *Scgb3a2* (ISH)/Ccsp (ISH)/calcitonin gene-related peptide (Cgrp), another NE cell marker (IHC), confirmed that cells in the pNEB microenvironment continue to express *Scgb3a2* at this stage and have low-to-negligible levels of Ccsp. Our data suggested that cells associated with NEBs are a distinct set of Clara cell progenitors.

High Levels of Uroplakin 3A Expression Distinguishes Secretory Precursors in the NEB Microenvironment. The absence of secretory cells in the airways of Notch signaling-deficient mice presented a unique opportunity to screen for additional markers enriched in the developing Clara cells. Thus, we compared the global gene expression profile of E18.5 lungs from control and mutant mice in which the *Rbpjk* gene was disrupted in the airway epithelium (*Shh-Cre;Rbpjk*$^{Flox/Flox}$ or *Rbpjk*^{cnull}) (8, 18). As expected, genes associated with the Clara cell phenotype, such as *Ccsp*, *Scgb3a2*, and *Cyp2f2*, were expressed at significantly higher levels in control lungs (Fig. 3*A*). A comprehensive description of this screen will be reported elsewhere. Importantly, this screen identified *Uroplakin 3a* (Upk3a; Fig. 3*A*) as a putative marker of Clara precursors. *Upk3a* encodes a single-pass transmembrane domain-containing protein of the Uroplakin family that is expressed in the urinary bladder epithelium (19, 20). Mice deficient in *Upk3a* have compromised urothelial permeability, but no phenotype has been described in the lung (19).

We examined *Upk3a* expression in control and *Rbpjk*^{cnull} mice by ISH (Fig. 3 *B* and *C*). In E18.5 controls, *Upk3a* was highly enriched in cell clusters in the proximal airways, although signals could be also detected at lower levels in scattered cells in the distal airway epithelium (Fig. 3*B*, bracket); this differed from the widespread expression patterns of *Scgb3a2* and Ccsp at E18.5 (Fig. 2). *Upk3a* signals were undetectable in airways of *Rbpjk*^{cnull} mice (Fig. 3*C*).

Developmental analysis of *Upk3a* expression using ISH and quantitative real-time PCR (qPCR) detected signals at E12.5 (qPCR) and 14.5 (ISH), and showed increasing levels thereafter (Fig. 3 *D–F*). ISH revealed clustered distribution from early stages and prompted us to investigate the relationship of *Upk3a*-expressing cells with pNEBs. Double ISH (*Upk3a*)/IHC (Ascl1) showed that *Upk3a*-expressing cells were juxtaposed to the Ascl1-labeled clusters from the earliest stages (Fig. 3 *E* and *F*). Quantitative analysis showed that 70–80% of pNEBs at E14.5 were associated with *Upk3a* clusters. Next we investigated whether *Upk3a*-expressing cells were present in the NEB microenvironment in the adult lung. Double ISH/IHC using a *Upk3a* riboprobe and an anti-Cgrp antibody showed at least 1–5 *Upk3a*-expressing cells in association with 50% of all NEBs examined (Fig. 3*G*).

Because *Cyp2f2* has been reported as a marker for Clara cells (17) and was also identified by our expression profiling as down-regulated in Notch-deficient airways, we characterized its developmental pattern of expression. ISH showed *Cyp2f2* expression throughout the epithelium of the trachea and extrapulmonary airways from E13.5 and expanded to distal airways at later times (Fig. S1 *A* and *B*). To determine the spatial relationships among *Scgb3a2*, *Upk3a*, *Cyp2f2*, and pNEBs, serial sections were labeled with these riboprobes and subsequently stained with an anti-Ascl1 antiserum. Analysis of E14.5 lungs showed that the pNEB-associated cell clusters that typically express strong *Scgb3a2* and *Upk3a* signals had little, if any, *Cyp2f2* (Fig. S1 *C–E*); this contrasted with the strong *Cyp2f2* signals in neighboring *Scgb3a2*-positive cells. At E18.5, this subpopulation could be distinguished by strong *Upk3a* but not by low *Cyp2f2* expression as seen at earlier times (Fig. S1*F*).

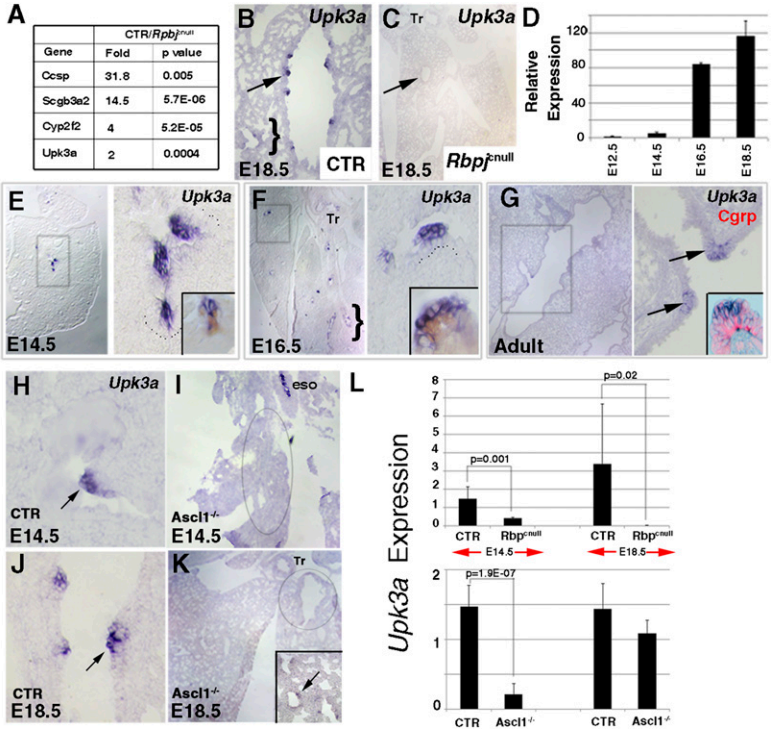

Fig. 3. High levels of *Upk3a* expression distinguishes Clara-like precursors in the pNEB microenvironment. (*A*) Profiling of E18.5 control and Notch signaling-deficient (*Rbpj*^{cnull}) lungs identified known markers for Clara cells and implicated *Upk3a* as a candidate marker. (*B* and *C*) ISH at E18.5 in control lungs revealed that *Upk3a* was highly enriched in clusters of cells in the proximal airways (*C*, arrow) and expressed at low levels in scattered cells in distal airways (*C*, bracket). No signal was detected along the airway axis in *Rbpj*^{cnull} airways (Tr, trachea). (*D*) qPCR analysis showed that *Upk3a* levels can be detected at E12.5 and increase throughout development. (*E* and *F*) *Upk3a* transcripts were detected by ISH from E14.5 onward in cell clusters juxtaposed to Ascl1-expressing cells (*E* and *F*; *Insets* show higher magnification). Some expression away from clusters was detected from E16.5 onward (*F*, bracket). *Upk3a* expression was also detected in a few cells in the adult airways (*G*, arrow) frequently juxtaposed to Cgrp-expressing NEBs (*G Inset*). (*H–K*) *Upk3a* expression was perturbed in Ascl1-null (Ascl1$^{-/-}$) lungs. Clusters of high *Upk3a* expression were detected in control at both E14.5 (*H*) and E18.5 (*J*), but not in mutant lungs at either time point [*I* and *K*, circled regions; note expression of Upk3A is detected in the esophagus in the mutant at E14.5 (*I*, eso)]. Rare *Upk3a*-expressing cells (nonclustered) could still be seen in the E18.5 Ascl1-null mutant (*K Inset*). (*L*) qPCR analysis of Upk3a expression in Rbpjk-deficient and Ascl1 mutants at E14.5 and E18.5 showing that Upk3a expression is dependent on both Notch signaling and Ascl1.

NEB Microenvironment Harbors a Subset of Clara Cell Precursors in Developing Airways. Next we asked whether the features identified in the pNEB-associated cells were dependent on the pNEBs. Previous studies show that neither solitary NE cells nor NEBs form in *Ascl1-null* mice (13, 15). Given the small numbers of cells in the pNEB microenvironment and paucity of specific markers for these cells, we reasoned that the ablation of these cells would have escaped detection, and reexamined *Ascl1*-null mice. Analysis of these mutants at E14.5 showed that, in the absence of pNEBs, the clustered expression of NICD and *Scgb3a2* was abolished, although the weak, nonclustered signals remained in proximal airways (Fig. S2 *A–D*). At E18.5, the strong expression of NICD and Scgb3a2 throughout the airway epithelium did not allow distinguishing differences between control and *Ascl1* mutants.

We then investigated the impact of *Ascl1* deletion on *Upk3a*. No *Upk3a*-labeled cell clusters were detected in *Ascl1*-null mutant lungs at E14.5 or E18.5 (Fig. 3 *H–K*). The selective loss of the *Upk3a*-labeled cell clusters was further supported by the presence of *Upk3a* signals in other structures (esophagus; Fig. 3*I*) or in the scattered cells outside the NEB microenvironment (Fig. 3*K*, *Inset*). The *Ascl1* phenotype contrasts with the generalized disruption of *Upk3a* that we found in the airways of $Rbpjk^{cnull}$ mice (Fig. 3*C*). qPCR showed that *Upk3a* mRNA is abolished in $Rbpjk^{cnull}$ lungs both at E14.5 and E18.5 (Fig. 3*L*). The observation is consistent with the inability to form Clara cells upon disruption of Notch signaling. In *Ascl1*-null mice, *Upk3a* expression was also markedly down-regulated at E14.5, but only marginally decreased at 18.5 (Fig. 3*L*). The more dramatic reduction in *Upk3a* transcripts seen at E14.5 mutants was expected because at this stage, *Upk3a*-expressing cells formed essentially around pNEBs. Later, the contribution of non–pNEB-associated cells minimized the differences in *Upk3a* expression between control and *Ascl1* mutants (see Fig. S2 *E–G* for Scgb3a2).

These results suggest that pNEBs are required to induce if not maintain a population of cells expressing high levels of *Upk3a* in its microenvironment.

The identification of *Upk3a* as a marker enriched in pNEB microenvironment provided us with an opportunity to examine the fate of these cells. We investigated the fate of *Upk3a*-expressing cells in the airways during prenatal and adult life using an $Upk3aCreER^{T2}$ transgenic mouse. A single dose of tamoxifen (*Materials and Methods* and Fig. 4*A*) was administered to $Upk3aCre\ ER^{T2}$;*Rosa26lacZ* dams 15.5 d postcoitum. Offspring were analyzed at E18.5 and at postnatal day 60. As putative Clara cell precursors, we investigated the ability of *Upk3aCre*-labeled cells to give rise to Clara and ciliated cells (2). Thus, we performed double-IHC/X-gal staining using antibodies against Foxj1, β-Tubulin IV (ciliated), and Ccsp, followed by quantitative analysis (Fig. 4). At E18.5, although lacZ signal was detected in a small number of cells, few were double-labeled with Ccsp, and only a single cell was double-labeled with Foxj1; this showed that the *Upk3a* lineage was largely uncommitted to either Clara or ciliated fates at this stage and was consistent with our IHC/ISH studies. In contrast, analysis of adult lungs showed labeling in both ciliated and Clara cells at nearly similar proportion (Ccsp: 47.2 ± 3.4%; β-Tubulin: 45.3 ± 4.0%; Fig. 4 *J* and *K*). The pool of cells that were lacZ positive; Ccsp negative and lacZ positive; β-Tubulin negative may include cells that remained undifferentiated even in adults. Lineage-labeled cells were distributed throughout the airway epithelium, and only a few of these cells were apposed to pNEBs (Fig. 4 *F* and *G*). Analysis using the NE marker PGP9.5 showed no colocalization with lacZ ($n = 69$ lacZ-positive cells). Together our data suggest that during development the pNEB microenvironment harbors a population of Clara-like precursors that generate both Clara and ciliated cells in adult life.

Notch Signaling Regulates Expression of Scgb3a2, Upk3a, and Ccsp by a Transcriptional Mechanism. To gain further insights into the mechanisms by which Notch signaling regulates gene expression in Clara progenitors, we examined the effect of loss or gain of Notch function on expression of genes at early stages, before the onset of

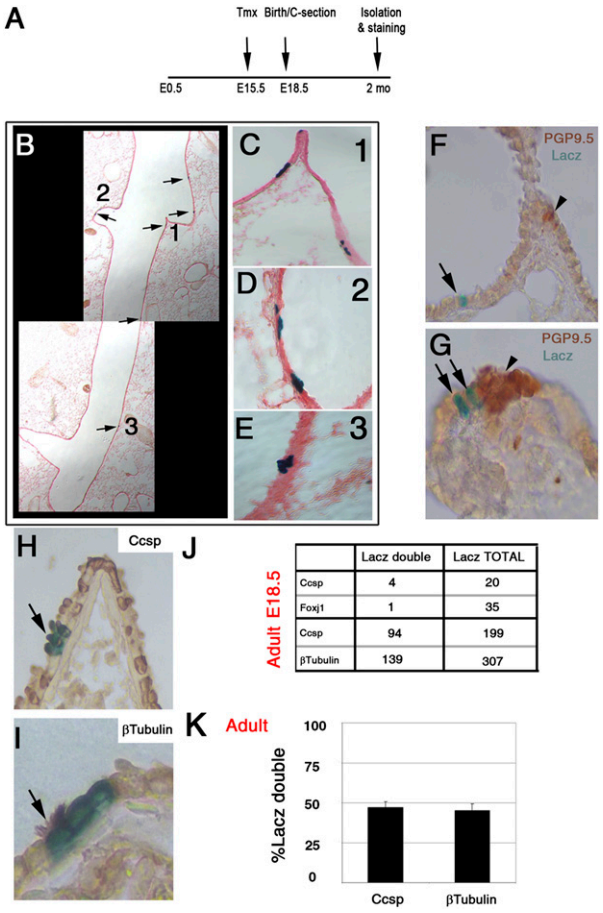

Fig. 4. Lineage analysis of Upk3a-expressing cells at E15.5 reveals that these cells are precursors of Clara and ciliated cells. (*A*) Experimental protocol for the induction and harvest of tissue from the $Upk3acreER^{T2} \times Rosa26lacz$. (*B–E*) Upk3a lineage-derived cells (blue) are distributed along the proximal/distal axis (counterstained with Fast Red) in clusters and as solitary cells (*B*, arrows). Regions 1, 2, and 3 in *B* are shown at higher magnification in *C–E*. (*F* and *G*) Double labeling of X-gal–stained preparations for PGP9.5 shows that Upk3a lineage-derived cells (arrows) are not in close association with NEBs (arrowheads), although rare examples of apposition are observed (*G*). Note that LacZ (arrow)- and PGP9.5 (arrowhead)- expressing cells are distinct. (*H* and *I*) Upk3a-expressing cells labeled at E15.5 contribute to Clara and ciliated lineages in adults. Double labeling of X-gal–stained preparations for Ccsp (*H*) and β-tubulin (*I*) demonstrate that these cells contribute to both Clara (*H*) and ciliated (*I*) lineages. (*J* and *K*) Quantitation of the numbers of X-gal–stained cells that co-label for Clara and ciliated markers at E18.5 (Ccsp, Foxj1, $n = 156$ airways) and in adults (Ccsp, β-Tubulin, $n = 501$ airways). The Upk3a lineage-derived cells are mostly uncommitted to either Clara or ciliated fates at E18.5 but differentiate into these lineages thereafter. *K*, mean ± SEM.

Ccsp expression. We generated mice in which Notch signaling was disrupted ($Rbpjk^{cnull}$) (18) or constitutively activated in the lung epithelium using ShhCre and *Rosa-NICD* transgenes (12). Analysis of the *Scgb3a2* pattern in E14.5 $Rbpjk^{cnull}$ lungs showed marked down-regulation in extrapulmonary airways and negligible signals in intrapulmonary airways, including the cells in the pNEB microenvironment, which normally express strong *Scgb3a2* (Fig. 5 *A* and *B* and Fig. 2). In contrast, E14.5 *ShhCreNICD* mice showed widespread expression of *Scgb3a2* in the airway progenitors (Fig. 5*E*). *Upk3a* expression was similarly modulated by Notch signaling (Fig. 5 *B* and *F*). We did not detect expression of *Ccsp* in E14.5 lungs overexpressing NICD, but strong signals were present at E18.5 (Fig. S3 *A* and *B*). As evidenced by the morphology, NICD overexpression led to aberrantly enlarged airways. Nevertheless,

DEVELOPMENTAL BIOLOGY

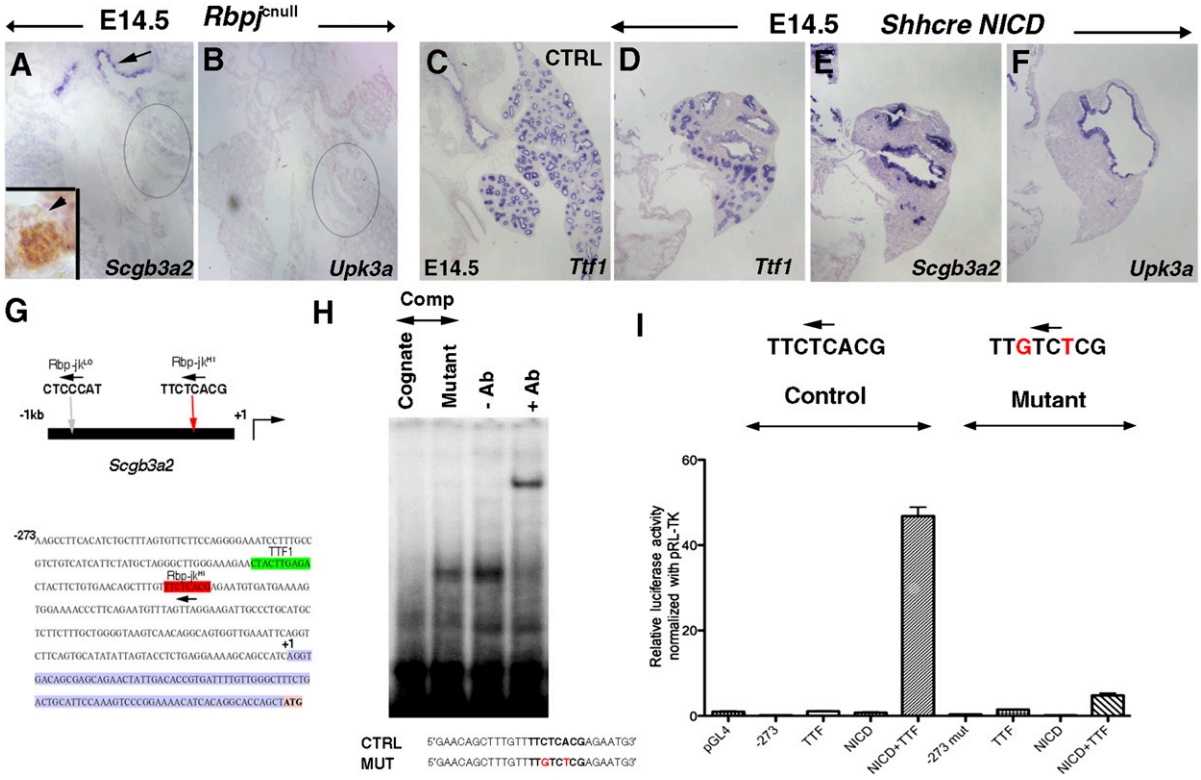

Fig. 5. Notch-dependent regulation of secretory cell-associated genes. (*A–F*) Analysis of Notch gain and loss of function in E14.5 airways in vivo. (*A* and *B*) Disruption of Notch signaling in *Rbpj*^{cnull} mutants disrupts expression of *Scgb3a2* and *Upk3a*. Comparable segments of the intrapulmonary airways in *A* and *B* (encircled by gray lines) evidence negligible expression of both markers in *Rbpj*^{cnull} lungs. Residual low-level expression of *Scgb3a2* was detected in the extrapulmonary airways of mutants only after prolonged staining (*A*, arrow). Double-*Scgb3a2* ISH/AscII IHC shows that specification of pNEBs was unaffected in *Rbpj*^{cnull} mutants, but no *Scgb3a2* was detected in surrounding cells (*A Inset*, arrowhead). (*C–F*) Shh cre-driven NICD perturbed lung architecture (compare distribution of *Ttf1* in *C* and *D*) and resulted in widespread expression of *Scgb3a2* and *Upk3a*. (*G* and *H*) In vitro analysis of the role of Notch signaling in the regulation of the *Scgb3a2* promoter. (*G*) Schematic showing presumptive Rbpjk binding sites (high-affinity site, red arrow; low-affinity site, gray arrow) in the *Scgb3a2* promoter 1 kb upstream to the transcription start site. (*G Lower*) Sequence of a −273-bp fragment of the *Scgb3a2* promoter showing putative Rbpjk (red) and TTF1 (green) binding sites. (*H*) Validation of the predicted high-affinity Rbpjk binding site in the Scgb3a2 promoter by EMSA. An anti-Rbpjk antibody supershifted the labeled oligonucleotide containing the putative high-affinity binding site (CTRL, lane +ab). Note that the band that is supershifted by anti-Rbpjk was competed by coincubation of the labeled oligonucleotide with an unlabeled CTRL oligonucleotide (cognate) but not competed by coincubation with an unlabeled mutant oligonucleotide lacking the high-affinity binding site (MUT, sequences shown below). (*I*) Luciferase assay examining the sufficiency of NICD and Ttf1 in the transactivation of the *Scgb3a2* promoter. NICD expression alone did not significantly transactivate the *Scgb3a2* promoter, but coexpression of NICD and Ttf1 synergistically up-regulated reporter expression. This synergistic up-regulation was abolished when the high-affinity Rbpjk binding site was mutated (−273mut; *G*).

these airways retained respiratory identity as they expressed *Ttf1* (Fig. 5 *C* and *D*).

Based on the genetic data above and our evidence establishing *Scgb3a2* as an early Clara marker, we investigated whether Notch could directly regulate *Scgb3a2* transcription. A screen for Rbpjk binding sites 1-kb region upstream to the transcription start site (TSS) of the murine *Scgb3a2* promoter revealed high (YGTGRGAA)- and low (RTGRGAR)-affinity binding sites (Fig. 5*G*) (21–23). For subsequent analysis we focused on the putative high-affinity binding site. We performed EMSA using COS-1 cell nuclear extracts and oligonucleotides containing the *Rbpj*k high-affinity binding sequence (intact, mutated); COS-1 cells are known to endogenously express Rbpjk (24). Detection of a DNA–protein band that was supershifted with an anti-Rbpj antibody confirmed that endogenous *Rbpj*k can bind to this site (Fig. 5*H*). Next, we performed luciferase reporter assays using *Scgb3a2* promoter sequences −273 bp to the TSS containing either a control (WT) or a mutated Rbpjk high-affinity site. Cotransfection with an NICD-containing plasmid resulted in minimal induction of reporter activity (<twofold). This response was similar to that elicited by cotransfection of the same construct with an expression plasmid-containing *Ttf1*, a known transcriptional regulator of *Scgb3a2*. We conclude that despite the presence of a high-affinity binding site in the promoter fragment, NICD expression is insufficient to induce reporter expression (Fig. 5*I*).

Interactions between Notch and other transcription factors have been implicated in the control of gene expression during development (21, 25). Moreover, synergistic regulation of the mouse *Scgb3a2* gene by Ttf1 and other transcription factors, such as C/EBP, has been previously reported (26). We tested the possibility that NICD could act in concert with Ttf1 to transactivate the *Scgb3a2* promoter (Fig. 5*I*). Coexpression of Ttf1 and NICD dramatically increased reporter activity (over 40-fold). Importantly, introducing a mutation in the *Rbpj*k high-affinity site (TTCTCACG to TTGTCTCG) nearly abolished this synergistic interaction (Fig. 5*I*).

We extended our promoter analysis to other Clara cell-associated genes such as *Upk3a* and *Ccsp*. Both genes have multiple Rbpjk and Ttf1 binding sites in their promoters (Figs. S4 and S5). Reporter assays showed that both *Upk3a* and *Ccsp* were transactivated by NICD and Ttf1 in a synergistic manner, as observed for *Scgb3a2* (Figs. S4 and S5). Together, our data suggest a model in which Notch, in conjunction with locally expressed transcription factors such as Ttf1, regulates gene transcription in Clara cell progenitors.

Discussion

In this study we examined how Notch influences Clara cell fate specification in airway progenitors, and the influence of local microenvironment in generating diversity among Clara cell precursors during development. We identify expression of *Scgb3a2* and Notch activation as early events in a program of Clara cell differentiation. Our in vitro assays show that Notch activation alone has a minimal effect in the transactivation of genes in Clara cell progenitors but is highly effective when combined with Ttf1. This context dependency is of biological significance because genetic studies have shown that Ttf1 is critical for the overall induction of respiratory cell fate, including secretory Clara cells (27, 28).

Ultrastructural studies of the developing airways show the pNEB microenvironment contains a distinct population of non-neuroendocrine, nonciliated cells (5). Here we report that this population of pNEB-associated epithelial cells can be distinguished in molecular terms by the expression of markers associated with Clara cells such as NICD, *Scgb3a2*, *Upk3a*, *Cyp2f2*, and Ccsp. Based on the marker that is most enriched and best distinguishes this population of cells, *Upk3a*, we undertook a lineage study to trace their fate in *Upk3aCreER^{T2};Rosa26 lacZ* mice. We find that labeling at E15.5 results in lacZ expression in both Clara and ciliated cells of the adult airways at nearly the same proportion. Moreover, this lineage did not contribute to NE cells. Thus, our studies demonstrate that the *Upk3a*-expressing cells, despite expressing little Ccsp, exhibit the properties of a Clara progenitor and implicate the pNEB microenvironment as a niche for Clara cell progenitors. It is likely that pNEBs are critical to specify or maintain the features of this subpopulation; however, the identification of the pNEB signals that mediate this process is beyond the scope of this work. Candidate signals present in NE cells potentially involved in these interactions include the Delta-like family of Notch ligands, or other currently uncharacterized Ascl1 targets (15). Interestingly, lineage analysis of *Scgb1a1CreER;R26YFP* mice demonstrates that Clara cells labeled in adulthood are more able to generate ciliated cells than Clara cells labeled at E18.5 (2). The identification of the Upk3a lineage-derived Clara cells could account for this difference. Whether the Upk3a-derived Clara cells that remain uncommitted during the embryonic period have a higher propensity to generate ciliated cells in adulthood remains to be determined.

The spatiotemporal pattern of *Scgb3a2* we describe in murine airways, including its enrichment in clusters in the pNEB microenvironment, is highly reminiscent of the CCSP pattern reported in developing airways of humans (29). Although SCGB3A2 has been reported in human neonatal lungs, no information is available on its pattern at early developmental stages in humans (14). A number of human conditions are associated with abnormal increase in NE bodies, including neuroendocrine hyperplasia of infancy (NEHI), diffuse idiopathic pulmonary neuroendocrine cell hyperplasia, and bronchopulmonary dysplasia (BPD). The aberrant expansion of neuroepithelial cells in these conditions is likely to have a profound impact in the local microenvironment, as shown by the increase in the NEB-associated clusters of CCSP-expressing cells in BPD lungs (29). Thus, further studies to better understand the mechanisms and consequences of the cellular interactions in this microenvironment have potentially high clinical significance.

Materials and Methods

A detailed description of the reagents and methodologies (mouse models, ISH, IHC, real-time PCR, EMSA, site-directed mutagenesis, DNA transfections, and luciferase reporter assays) used in this work can be found in *SI Materials and Methods*.

ACKNOWLEDGMENTS. We thank FengZhi Shao for technical assistance, and Mike Kirber, Narmada Khare, and members of W.V.C.'s laboratory and the Lung Development Group at the Pulmonary Center, Boston University Medical Center (BUMC), for helpful discussions. We also thank Raphael Kopan and Mitsuru Morimoto for thought-provoking discussion and detailed comments on the manuscript. This work was funded by National Institutes of Health National Heart, Lung, and Blood Institute Grants P01 HL47049 and R01 HL105971 (to W.V.C.) and a BUMC start-up grant (to A.G.).

1. Rawlins EL, et al. (2008) Epithelial stem/progenitor cells in lung postnatal growth, maintenance, and repair. *Cold Spring Harb Symp Quant Biol* 73:291–295.
2. Rawlins EL, et al. (2009) The role of Scgb1a1+ Clara cells in the long-term maintenance and repair of lung airway, but not alveolar, epithelium. *Cell Stem Cell* 4: 525–534.
3. Reynolds SD, Malkinson AM (2010) Clara cell: Progenitor for the bronchiolar epithelium. *Int J Biochem Cell Biol* 42:1–4.
4. Stripp BR, Maxson K, Mera R, Singh G (1995) Plasticity of airway cell proliferation and gene expression after acute naphthalene injury. *Am J Physiol* 269:L791–L799.
5. Hung KS (1982) Development of neuroepithelial bodies in pre- and postnatal mouse lungs: Scanning electron microscopic study. *Anat Rec* 203:285–291.
6. Reynolds SD, Giangreco A, Power JH, Stripp BR (2000) Neuroepithelial bodies of pulmonary airways serve as a reservoir of progenitor cells capable of epithelial regeneration. *Am J Pathol* 156:269–278.
7. Morimoto M, et al. (2010) Canonical Notch signaling in the developing lung is required for determination of arterial smooth muscle cells and selection of Clara versus ciliated cell fate. *J Cell Sci* 123:213–224.
8. Tsao PN, et al. (2009) Notch signaling controls the balance of ciliated and secretory cell fates in developing airways. *Development* 136:2297–2307.
9. Artavanis-Tsakonas S, Rand MD, Lake RJ (1999) Notch signaling: Cell fate control and signal integration in development. *Science* 284:770–776.
10. Lai EC (2004) Notch signaling: Control of cell communication and cell fate. *Development* 131:965–973.
11. Ilagan MX, Kopan R (2007) SnapShot: Notch signaling pathway. *Cell* 128:1246.
12. Guseh JS, et al. (2009) Notch signaling promotes airway mucous metaplasia and inhibits alveolar development. *Development* 136:1751–1759.
13. Ito T, et al. (2000) Basic helix-loop-helix transcription factors regulate the neuroendocrine differentiation of fetal mouse pulmonary epithelium. *Development* 127:3913–3921.
14. Reynolds SD, Reynolds PR, Pryhuber GS, Finder JD, Stripp BR (2002) Secretoglobins SCGB3A1 and SCGB3A2 define secretory cell subsets in mouse and human airways. *Am J Respir Crit Care Med* 166:1498–1509.
15. Borges M, et al. (1997) An achaete-scute homologue essential for neuroendocrine differentiation in the lung. *Nature* 386:852–855.
16. Jain R, et al. (2010) Temporal relationship between primary and motile ciliogenesis in airway epithelial cells. *Am J Respir Cell Mol Biol* 43:731–739.
17. Zemke AC, et al. (2009) Molecular staging of epithelial maturation using secretory cell-specific genes as markers. *Am J Respir Cell Mol Biol* 40:340–348.
18. Tsao PN, et al. (2008) Gamma-secretase activation of notch signaling regulates the balance of proximal and distal fates in progenitor cells of the developing lung. *J Biol Chem* 283:29532–29544.
19. Hu P, et al. (2000) Ablation of uroplakin III gene results in small urothelial plaques, urothelial leakage, and vesicoureteral reflux. *J Cell Biol* 151:961–972.
20. Liang FX, et al. (2001) Organization of uroplakin subunits: Transmembrane topology, pair formation and plaque composition. *Biochem J* 355:13–18.
21. Schwanbeck R, Martini S, Bernoth K, Just U (2011) The Notch signaling pathway: Molecular basis of cell context dependency. *Eur J Cell Biol* 90:572–581.
22. Ong CT, et al. (2006) Target selectivity of vertebrate notch proteins. Collaboration between discrete domains and CSL-binding site architecture determines activation probability. *J Biol Chem* 281:5106–5119.
23. Morel V, Schweisguth F (2000) Repression by suppressor of hairless and activation by Notch are required to define a single row of single-minded expressing cells in the Drosophila embryo. *Genes Dev* 14:377–388.
24. Lu FM, Lux SE (1996) Constitutively active human Notch1 binds to the transcription factor CBF1 and stimulates transcription through a promoter containing a CBF1-responsive element. *Proc Natl Acad Sci USA* 93:5663–5667.
25. Bray S, Bernard F (2010) Notch targets and their regulation. *Curr Top Dev Biol* 92: 253–275.
26. Tomita T, et al. (2008) CAATT/enhancer-binding proteins alpha and delta interact with NKX2-1 to synergistically activate mouse secretoglobin 3A2 gene expression. *J Biol Chem* 283:25617–25627.
27. Kimura S, et al. (1996) The T/ebp null mouse: Thyroid-specific enhancer-binding protein is essential for the organogenesis of the thyroid, lung, ventral forebrain, and pituitary. *Genes Dev* 10:60–69.
28. Minoo P, Su G, Drum H, Bringas P, Kimura S (1999) Defects in tracheoesophageal and lung morphogenesis in Nkx2.1(–/–) mouse embryos. *Dev Biol* 209:60–71.
29. Khoor A, Gray ME, Singh G, Stahlman MT (1996) Ontogeny of Clara cell-specific protein and its mRNA: Their association with neuroepithelial bodies in human fetal lung and in bronchopulmonary dysplasia. *J Histochem Cytochem* 44: 1429–1438.